

# Multi-muon events at the Tevatron: a hidden sector from hadronic collisions

Riccardo Barbieri<sup>a</sup>, Lawrence J. Hall<sup>b</sup>,  
Vyacheslav S. Rychkov<sup>a</sup> and Alessandro Strumia<sup>c</sup>

<sup>a</sup> *Scuola Normale Superiore and INFN, Piazza dei Cavalieri 7, 56126 Pisa, Italy*

<sup>b</sup> *Department of Physics, University of California, Berkeley, and  
Theoretical Physics Group, LBNL, Berkeley, CA 94720, USA*

<sup>c</sup> *Dipartimento di Fisica dell'Università di Pisa and INFN, Italia*

## Abstract

We show an explicit attempt to interpret the multi-muon anomaly recently claimed by the CDF collaboration in terms of a light scalar singlet  $\phi$  which communicates with the standard quarks either through a heavy scalar or a heavy fermion exchange. Building on arXiv:0810.5730, that suggested a singlet  $\phi$  with a chain decay into a final state made of four  $\tau\bar{\tau}$  pairs, we can simulate most of the muon properties of the selected sample of events. Some of these properties adhere rather well to the already published data; others should allow a decisive test of the proposed interpretation. Assuming that the test is positively passed, we show how the PAMELA excess can be fitted by the annihilation of a TeV Dark Matter particle that communicates with the Standard Model via the new light singlet(s).

# 1 Introduction and statement of the problem

The CDF Collaboration has recently published a study of a significant sample of multi-muon events with unexpected properties [1]. The D0 Collaboration performed a similar search without finding similar events [2]. While it is still possible that these events will be in the end accounted for in terms of standard physics and detector effects, yet a small but significant fraction of them has characteristics which are peculiar enough to deserve attention. This has in fact prompted a phenomenological conjecture [3] that tries to explain them in terms of new physics: the pair production of a relatively light Standard Model singlet,  $\phi$ , each with a cascade decay into a final state made of 8 tau leptons. An intriguing feature of this *explanation* is that it describes well the sign-coded multiplicity distribution of the additional muons, from two on, found in a cone<sup>1</sup> around the direction of a primary muon. In this interpretation, such a distribution is simply related, given the detector efficiencies in muon identification, to the  $\tau \rightarrow \mu$  decay probability. On the other hand, the apparent difficulty in exhibiting a plausible production mechanism of the  $\phi$ -pair casts doubts on the significance of the proposal and, even more importantly, prevents a decisive comparison of the model with the data. In spite of its uncertainties and ambiguities, this situation motivates us to try to go further.

A main problem one faces right at the beginning is how to select, from the overwhelming number of background events, those ones that may represent the signal. Secondly, a proper understanding of the event properties that involve hadronic tracks requires a detection simulation that we cannot do. To get around these problems we adopt the following strategy. We first concentrate our attention on a sub-class of about 4000 events that contain at least two muons (i.e. one primary and at least one additional) in each of the two cones. These events have also been highlighted in [1, 3] and found to have several properties especially difficult to understand in terms of known physics. We assume that these events constitute *the signal* and we seek for a production mechanism of the  $\phi$ -pair that can account for the measured properties of the muons contained in them. Out of all possibilities, discussed in Section 2, somewhat surprisingly one single effective operator of dimension 5 fits the invariant mass distribution of all muons in this sample for a definite value of its scale. The operator is of the form  $\bar{q}q\phi^2$ , where  $q$  is a first generation quark.

Encouraged by this result, which fixes the production mechanism, we analyze in Section 3 a few other measured features of the multi-muon events: the  $\mu^\pm$  multiplicity, impact parameter and invariant mass of muons in one cone. Given our definition of the signal, the background can be clearly identified. We show that it should be possible, with the data at hand, to fit the tail of the muon impact parameter distribution by adopting the chain decay model proposed in [3],  $\phi \rightarrow 2\phi_1 \rightarrow 4\phi_2$ , where  $\phi_{1,2}$  are two other SM singlets and  $\phi_2$  decays into a tau pair with a lifetime around 30 picoseconds. Our main purpose is to make possible a close comparison of the model with the data so as to allow a decisive test. To this end we discuss in Section 4 a few quantitative predictions of the model that should be compared with the data.

---

<sup>1</sup>The events in question are triggered by a pair of muons with  $p_T > 3$  GeV and  $|\eta| < 0.7$ . Additional muons with  $p_T > 2$  GeV and  $|\eta| < 1.1$ , which are often present in these events, are grouped into two *cones* of opening angle  $36.8^\circ$  around the directions of the trigger (also called *primary*) muons. Muons which happen to lie outside of these cones are ignored.

The  $\phi$ -pair production cross section needed to explain *the signal* is about 200 pb, in turn requiring a scale of the effective operator that describes it of about 100 GeV. To make it acceptable, we find it necessary to *deconstruct* the effective operator in terms of renormalizable interactions, with new particles mediating the communication between the quarks in the proton and the *hidden* sector that contains  $\phi$ . These new particles and interactions must not lead to any unseen structure in the multi-muon data and must be consistent with known experimental constraints. Given the size of the cross section and the low effective scale involved, this proves nontrivial to achieve. Nevertheless we illustrate in Section 5 two minimal models that can pass the test, to the best that we can tell. One involves a scalar exchange in the  $s$ -channel and another a fermion exchanged in the  $t$ -channel. In both cases the couplings to the singlet  $\phi$  saturate perturbation theory. We also briefly comment on the problems that one may face in turning them into complete satisfactory extensions of the SM.

If this interpretation of the CDF events will resist a further scrutiny along the lines we are proposing, the existence of the light scalar sector suggests a connection with recent astro-particle data. In Section 6 we consider a hidden-sector Dark Matter model where DM annihilations into  $\phi$ 's that decay into  $\tau$ 's can provide the positron excess claimed in  $e^+$  cosmic rays by PAMELA [4], while giving in the  $e^+ + e^-$  spectrum a feature somewhat smoother than the peak claimed by ATIC [5]. Conclusions are summarized in Section 7.

## 2 The production of the *signal* events

As mentioned, we first concentrate our attention on the events with two cones containing at least two muons each, which we call *signal* events as their features are peculiar enough that they should be minimally polluted by known backgrounds and could therefore be a quasi-pure sample of a beyond the SM signal. For an integrated luminosity of  $2.1 \text{ fb}^{-1}$  there are about four thousand such events [1]. If they have to arise from  $\phi \rightarrow 4\tau\bar{\tau}$ , this requires a significant  $p\bar{p} \rightarrow \phi\phi$  cross section, above 100 pb. Furthermore the invariant mass distribution of all muons contained in these events, Fig. 35a of [1], which we aim to explain, does not show any special feature other than a threshold rise and an extended tail. In view of this we are led to consider an effective operator bilinear in  $\phi$  and with two gluons or a quark-antiquark pair. There are three such operators of dimension less or equal to 6<sup>2</sup>:

$$O_5 = \frac{1}{\Lambda}(\bar{q}q)|\phi|^2, \quad O_{6F} = \frac{1}{\Lambda^2}(\bar{q}\gamma_\mu q)(\phi^* \overleftrightarrow{\partial}_\mu \phi), \quad O_{6G} = \frac{1}{\Lambda^2}G_{\mu\nu}^a G_{\mu\nu}^a |\phi|^2, \quad (2.1)$$

where  $q$  is a quark field, either  $u$  or  $d$ , and  $G$  the gluon field. We will normalize our plots below assuming that  $O_5$  couples only to  $u$ , while  $O_{6F}$  couples to both  $u$  and  $d$  with equal strength.

With the amplitude corresponding to each of these operators, we have simulated the  $\phi$ -pair production followed by the decay chain

$$\phi \rightarrow 2 \phi_1 \rightarrow 4 \phi_2 \rightarrow 8 \tau \quad (2.2)$$

---

<sup>2</sup>For definiteness, we assume that  $\phi$  is a complex field.

with  $m_\phi = 15$  GeV; see [3] and Section 3 for a discussion of this choice. Imposing the experimental cuts and detection efficiencies<sup>3</sup> we get for each of the above operators the signal cross section<sup>4</sup>:

$$\sigma_5 = 0.38 \text{ pb} \left( \frac{200 \text{ GeV}}{\Lambda} \right)^2, \quad \sigma_{6F} = 1.3 \text{ pb} \left( \frac{200 \text{ GeV}}{\Lambda} \right)^4, \quad \sigma_{6G} = 0.52 \text{ pb} \left( \frac{200 \text{ GeV}}{\Lambda} \right)^4.$$

For reference the total  $p\bar{p} \rightarrow \phi\phi^*$  cross sections (without imposing cuts and efficiencies) are

$$\sigma_{5,\text{tot}} = 220 \text{ pb}, \quad \sigma_{6F,\text{tot}} = 105 \text{ pb}, \quad \sigma_{6G,\text{tot}} = 370 \text{ pb} \quad \text{for } \Lambda = 200 \text{ GeV}.$$

Fig. 1 shows how well each of these three production models can account for the experimental distribution of the invariant mass of all muons contained in the two signal cones, shown in Fig. 35a of [1]. The hardness of the observed distribution motivated us to consider production via effective non-renormalizable operators. The single relevant parameter here is the effective scale attached to each individual operator. We find it remarkable that a single operator,  $O_5$ , can fit the full distribution. For definiteness we take  $q = u$  only, which requires  $\Lambda = 85$  GeV (fixed in this case to reproduce the total number of events). On the other hand  $O_{6F}$  and  $O_{6G}$  can separately reproduce only the tail and the low-mass region close to threshold, respectively.

The dashed red line in Fig. 1a shows the spectrum shape which results if  $\phi\phi^*$  are decay products of a narrow 300 GeV scalar resonance:  $q\bar{q} \rightarrow S \rightarrow \phi\phi^*$  (in arbitrary normalization). The purpose of including this spectrum, clearly unable to reproduce the experimental data, is twofold. First, this case was considered in [3], and our simulations agree. Second, since the 300 GeV  $S$ -exchange gives a spectrum peaked around 30 GeV, we can deduce that muons carry on average around 1/10 of the total  $\phi\phi^*$  invariant mass. In particular, events at the tail of the experimental spectrum,  $M_{\text{muons}} \sim 100$  GeV, should correspond to  $\sqrt{\hat{s}} \sim 1$  TeV.

### 3 Some measured properties of the multi-muons

Concentrating on the  $\phi$ -production described by  $O_5$  with  $\Lambda$  fixed at 85 GeV, we here try to reproduce a few other significant properties of the muons in the CDF events of [1]: 1) the already mentioned sign-coded multiplicity distribution; 2) the invariant mass of the muons in a single cone; 3) the muon impact parameter distribution. Notice that data of [1] about 1) and 3) also contain events outside the sub-sample discussed in Section 2 that we view as signal events; thereby we allow for the presence of a background.

---

<sup>3</sup>Trigger muons must have transverse momentum  $p_T > 3$  GeV, rapidity  $|\eta| < 0.7$ , and are detected with efficiency  $p_{\text{eff}} = 0.44$ ; additional muons must have  $p_T > 2$  GeV,  $|\eta| < 1.1$  and  $p_{\text{eff}} = 0.838$ . Furthermore, the invariant mass of the trigger muon pair must be between 5 and 80 GeV; the relative azimuthal angle for the opposite sign trigger muon pair must be below 3.135 radians.

<sup>4</sup>Our simulations were performed by adding the necessary new particles and processes in PYTHIA 8.108 [6] and were cross-checked with the help of home-grown Monte-Carlo programs written in MATHEMATICA (both stand-alone and passing Les Houches events to PYTHIA for parton shower).

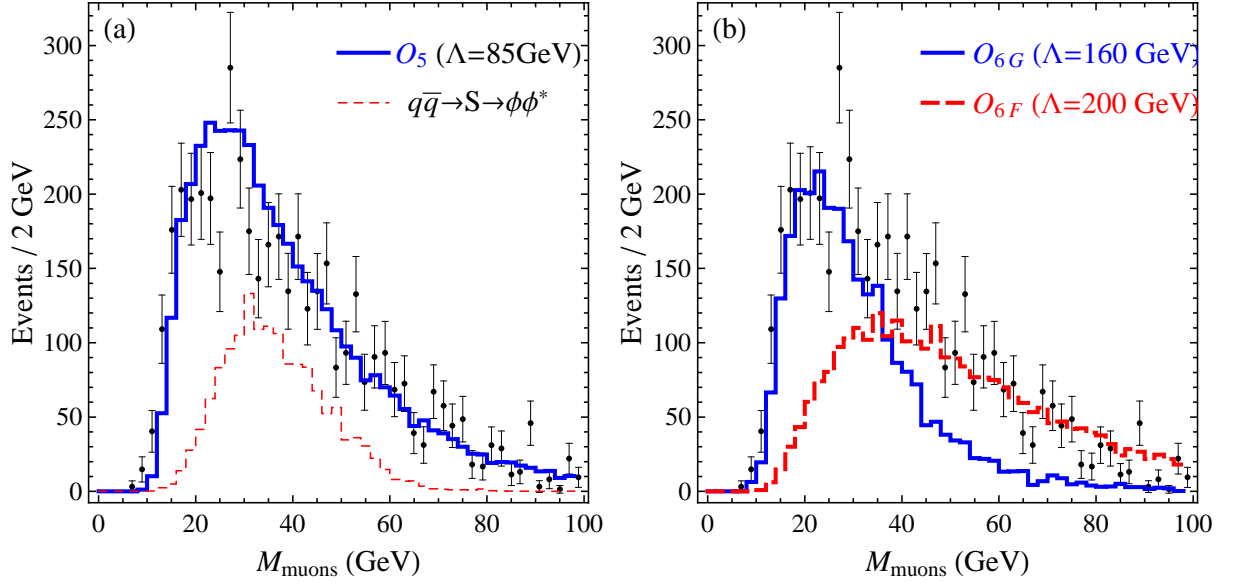


Figure 1: The invariant mass of all muons in events with at least two muons in both cones. The experimental data are from Fig. 35a of [1],  $L_{int} = 2.1 \text{ fb}^{-1}$ .

### 3.1 Sign-coded muon multiplicity

For reasons of graphical illustration, the sign-coded muon multiplicity  $\mathcal{M}$  is defined for each of the two  $36.8^\circ$  cones around the trigger muons by the formula

$$\mathcal{M} = N_{OS} + 10N_{SS}$$

where  $N_{OS}$  ( $N_{SS}$ ) is the number of additional muons in the cone having opposite (same) sign as the trigger muon. Thus e.g.  $\mathcal{M} = 0$  corresponds to cones without additional muons. In Table 1 and Fig. 2 we compare the data with our simulation.

The shape of this distribution is largely independent of the production mechanism, and indeed our Fig. 2 is quite similar to Fig. 1 of [3]. Since we have fixed the production mechanism (the  $O_5$  operator), we can simulate not only the shape but also the absolute normalization ( $\Lambda = 85 \text{ GeV}$ ), while in Fig. 1 of [3] normalization has been fixed arbitrarily. We see in particular that we can reproduce essentially all events (within errors) with 3 or more muons in a cone: only a relatively small systematic excess of not understood backgrounds is here possibly needed to fully account for the event rates. However, only about a third of events with 2 muons in a cone is reproduced. Since we fixed the normalization by using the events with two or more muons in *both* cones, this shows that events with only 2 muons in one cone and 1 muon in the other are still significantly contaminated by backgrounds.

The fraction of events without additional muons that we are able to reproduce is negligible. Almost all of these events must be background. Indeed according to [1] at least 50% of events without additional muons can be due to in-flight decays of kaons and hyperons producing real muons or pion punchthroughs.

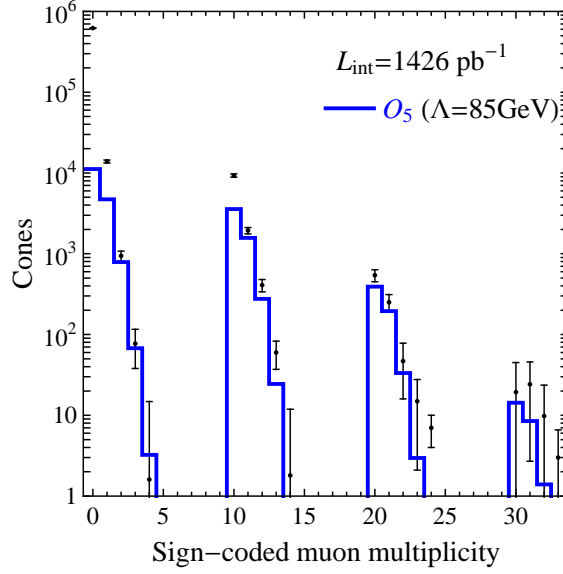


Figure 2: Comparison of our production model with the experimental data (Fig. 22b of [1], significant part only). Every cone enters separately into this histogram (thus every event enters twice).

$\mathcal{M}$	Cone content	Experiment	$O_5(\Lambda = 85\text{GeV})$
00	$\pm$	$620307 \pm 3413$	11184
01	$\pm \mp$	$13880 \pm 573$	4722
02	$\pm \mp \mp$	$941 \pm 135$	790
03	$\pm \mp \mp \mp$	$77 \pm 39$	68
04	$\pm \mp \mp \mp \mp$	$1.6 \pm 13.2$	3
10	$\pm \pm$	$9312 \pm 425$	3580
11	$\pm \pm \mp$	$1938 \pm 173$	1573
12	$\pm \pm \mp \mp$	$409 \pm 71$	277
13	$\pm \pm \mp \mp \mp$	$60 \pm 23$	24
20	$\pm \pm \pm$	$542 \pm 91$	392
21	$\pm \pm \pm \mp$	$251 \pm 61$	194
22	$\pm \pm \pm \mp \mp$	$47 \pm 31$	33
23	$\pm \pm \pm \mp \mp \mp$	$14.9 \pm 12.8$	3
30	$\pm \pm \pm \pm$	$19.4 \pm 25.6$	14
31	$\pm \pm \pm \pm \mp$	$24.2 \pm 21.5$	8
32	$\pm \pm \pm \pm \mp \mp$	$9.8 \pm 13.8$	1

Table 1: Numerical content of Fig. 2. Experimental data taken from Table X of [1] (significant part only). The data correspond to  $L_{\text{int}} = 1426 \text{ pb}^{-1}$ . The statistical errors of our simulation ( $\sim 0.2\sqrt{N_{\text{bin}}}$ ) are negligible compared to the experimental errors.

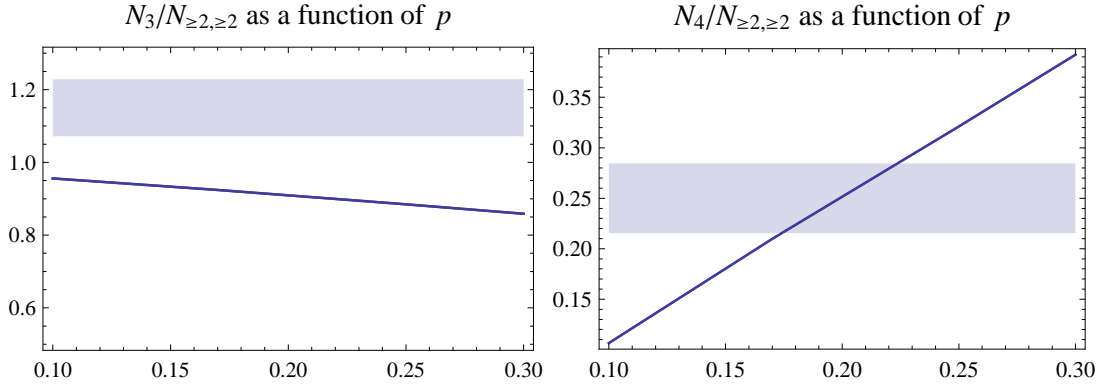


Figure 3: *The numbers of events with 3 muons in a cone  $N_3$  (the sum of bins 02,11,20 in Table 1) and with 4 muons in a cone  $N_4$  (the sum of bins 03,12,21,30) relative to the number of events with at least two muons in each cone  $N_{\geq 2, \geq 2}$ , simulated as a function of the varying  $\tau \rightarrow \mu$  branching ratio  $p$ . The bands show experimental values. The physical value  $p = 0.17$  gives reasonable agreement in both plots. One can see that the ratio  $N_3/N_{\geq 2, \geq 2}$  is rather insensitive to the variation of  $p$ , while the ratio  $N_4/N_{\geq 2, \geq 2}$  prefers the values of  $p \sim 0.2$ , close to the physical value.*

Notice that the above agreement of simulation with experiment, in bins with  $\geq 3$  muons, relies on the precise value of  $p = \text{BR}(\tau \rightarrow \mu) \approx 0.17$ , thereby indirectly supporting the  $\tau$  interpretation. This can be seen by generating toy Monte-Carlos in which  $p$  varies in the  $0.1 \div 0.3$  range (while keeping fixed the muon detection efficiencies). The number of events with 3 muons in a cone (including sign-coding), relative to the events with at least two muons in both cones, is largely independent of  $p$ . This is not unexpected, since the probability to put 2 additional muons in the same cone is roughly the same as to put them in different cones. On the contrary, the relative number of events with 4 or more muons in a cone was quite sensitive to  $p$ , to the extent that  $p = 0.1(0.3)$  led to clear shortage(excess) of events in these bins, compared to experiment, see Fig. 3. At the same time the relative distribution of these events into the various sign-coded bins is determined by simple combinatorics and, as a result, proves to be insensitive to the variations of  $p$ .

### 3.2 Single cone muon invariant mass

The multi-muon events are characterized by low invariant mass of muons in a single cone, with a spectrum which sharply cuts off at  $2 \div 3$  GeV. It was shown in [3] that this cutoff can be reproduced within the hypothesis of the decay chain (2.2) if the mass of  $\phi$  is not much above the  $8\tau$  threshold (14.2 GeV). This conclusion is largely independent of the production mechanism, and in particular holds within our model. In Fig. 4 we compare the data with our simulation for  $m_\phi = 15$  and 17 GeV (for events where both cones contain at least 2 muons, i.e. the *signal* events of Section 2).

The overall normalization is fixed in both cases to reproduce the total number of events.

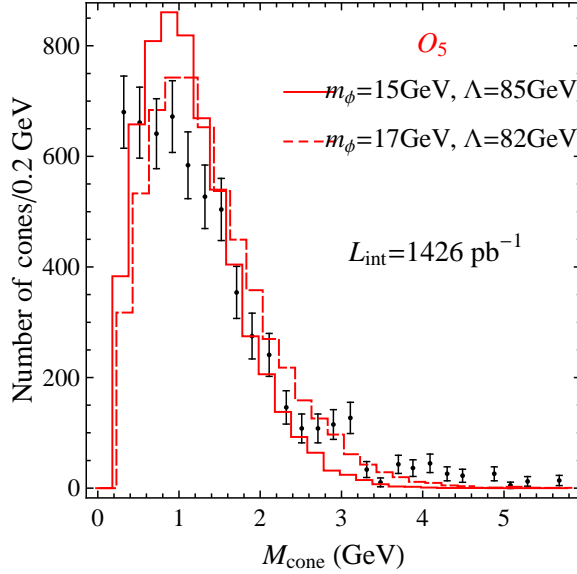


Figure 4: Invariant mass,  $M_{\text{cone}}$ , of all muons in a cone when both cones contain at least two muons. Data reproduced from Fig. 41a of [1].

While the data are reproduced in an acceptable way for these two masses, higher values (see [3] for  $m_\phi = 20$  GeV) start showing a clear deviation.

We however see that a discrepancy is present at small  $M_{\text{cone}}$ : while the data remain almost constant down to the lowest bin, the simulation drops there. The physical reason for this drop is intuitively clear: it corresponds to a small probability to have an almost collinear muon pair. Without a precise understanding of the detector (e.g. possible punch-through of hadrons mimicking muons) and of the statistical correlations between the various bins we cannot say more on this issue nor perform a precise  $\chi^2$  analysis.

It is legitimate to ask if the experimental distribution in Fig. 4 also contains a peak corresponding to the possible subdominant  $\phi_2$  decay channel, directly into muons,  $\phi_2 \rightarrow \mu^+\mu^-$ . Such a peak would have to be located at  $m_{\phi_2}$ , i.e. slightly above  $2m_\tau \simeq 3.55$  GeV<sup>5</sup>. Indeed we see some excess of events around this value of  $M_{\text{cone}}$  (which could become statistically significant with more statistics), but, at the same time, we do not forget an important source of dimuon pairs —  $c\bar{c}$  mesons — present in the  $3 \div 4$  GeV mass region. From the model-building point of view, the branching ratio  $\phi_2 \rightarrow \mu^+\mu^-$  may well be suppressed to an unobservable level (see Section 5).

### 3.3 The muon impact parameter

For a given charged particle track, the impact parameter  $d$  is defined as the distance between the track and the primary interaction vertex in the transverse plane, see Fig. 5.

One of the most striking properties of multi-muon events is that the impact parameter distribution of muon tracks has an exponential tail. Such a tail can be explained if the tracks originate

<sup>5</sup>And not at 7.2 GeV as in Fig. 1 of [7].



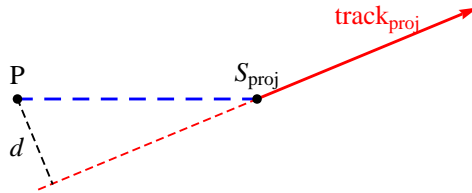


Figure 5: The impact parameter  $d$  is the distance between the track projection on the transverse plane  $\text{track}_{\text{proj}}$  and the primary interaction vertex  $P$ , which is experimentally known with high precision (in particular due to many soft hadronic tracks originating from it), while the secondary vertex  $S$  is not measured unless more than one track originates from it.

from decays of a long-lived particle. Notice that a boost  $\gamma$  of the decaying particle does not affect the typical value of the impact parameter, since it increases the typical decay distance  $\ell \sim \gamma c\tau_0$  but also decreases the typical collimation angle of decay products by the same factor  $\gamma$ . As a result the decay scale of the impact parameter distribution is of the order of the decaying particle's  $c\tau_0$ . The precise proportionality coefficient in general depends on the kinematic cuts.

In Fig. 6 we compare one of the several published impact parameter distributions (impact parameters of primary muons of all cones containing exactly 2 muons) with our simulation. We assume that  $\phi \rightarrow 2\phi_1 \rightarrow 4\phi_2$  decays are prompt, while  $\phi_2 \rightarrow \tau\bar{\tau}$  has a long lifetime. As discussed in [3], this assumption is forced on us by another piece of experimental data which we do not discuss here: no significant correlation between the impact parameters of different muonic tracks in the same cone.

We see that both the decay rate and the normalization of the exponential tail can be reproduced for a  $\phi_2$  lifetime around 30 ps.<sup>6</sup> Note that ‘naive’ decay exponent would give a 20 ps lifetime; the fact that the naive ultra-relativistic estimate underestimates the true lifetime by 30% in this particular case has already been noticed in [3] on the basis of a toy simulations. We also see that the large number of events at small  $d$  are not reproduced by our signal model. Most of these events must be due to QCD contributions, e.g. sequential  $b$  quark decays which had been subtracted in the distributions considered previously but not in Fig. 6. All data are extracted from [1], so that we follow their definitions.

## 4 Possibilities for further experimental tests

Now that a concrete proposal for the  $\phi$ -production via the  $O_5$  operator has emerged, what other possible tests could provide further checks of the model? Many such tests can be done using information about hadrons present in the multi-muon events. However, any study with hadrons would require detector simulation, especially because the relevant experimental information [1] involves hadronic *tracks* rather than, say, isolated jets.

<sup>6</sup>This value has to be taken with a grain of salt since the tail of the experimental distribution may be significantly contaminated by  $K_S^0$  in-flight decays (lifetime 90 ps).

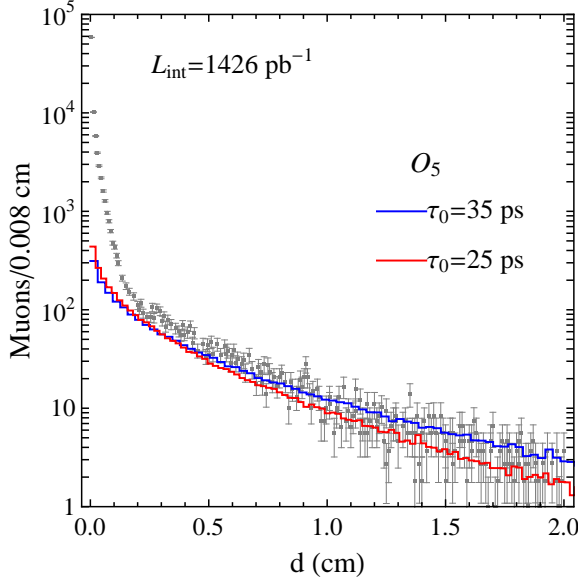


Figure 6: *Primary muon impact parameter distribution for cones containing exactly two muons. Data taken from Fig. 25a of [1].*

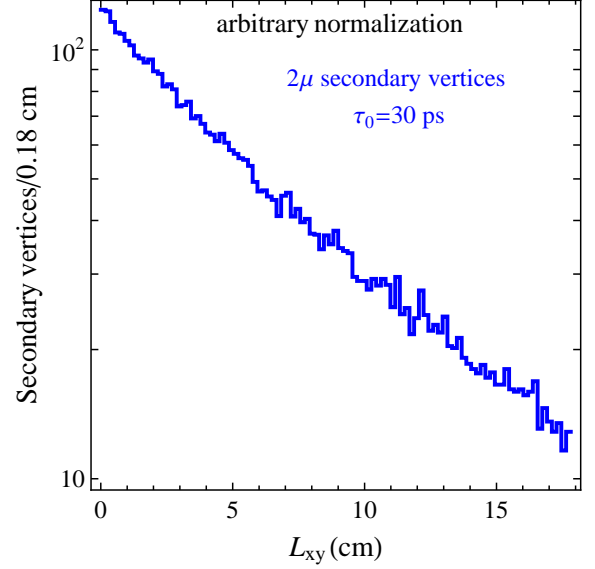


Figure 7: *The simulated distribution for  $L_{xy}$  for  $\tau_0 = 30$  ps and for dimuon secondary vertices (in arbitrary normalization).*

In this Section we discuss 3 further experimental tests which involve only muons and which might be relatively easier to implement. The corresponding experimental distributions are not yet available. These tests are: 1) dimuon displaced vertices; 2) muon track alignment; 3) deviation from back-to-backness in the CM frame of the hard process. *For illustrative purposes only* we will show in all cases the expected distributions from our simulation.

All our predictions below are computed using our simplified simulation of the triggering and reconstruction process, see footnote 1. In order to perform a precise comparison with the data, the predictions should be recomputed using the full simulation of the detector, available only to the experimental collaborations.

#### 4.1 Dimuon displaced vertices

If the model is right, a fraction of events must contain a displaced secondary vertex with two muon tracks originating from it. Such a vertex occurs when both taus in  $\phi_2 \rightarrow \tau\bar{\tau}$  decay into a muon. According to our simulation, for  $L_{\text{int}} = 2.1 \text{ fb}^{-1}$  there will be about 2000 such secondary vertices, for  $\phi_2$  lifetime of 30 ps almost all of them within the CDF inner silicon vertex detector (10.6 cm radius). Taking into account excellent tracking capabilities of the CDF detector, a significant fraction of these vertices should be identifiable.

A useful experimental quantity to describe the secondary vertex distribution is called  $L_{xy}$ , the distance between the secondary and primary event vertices projected onto the transverse momentum of the two-track system. In Fig. 7 we give our simulated distribution for  $L_{xy}$  when

the secondary vertex is determined by two muon tracks.

## 4.2 Muon track alignment

As discussed in Section 3,  $m_\phi$  cannot be much above  $15 \div 17$  GeV. On the other hand we must have  $m_{\phi_2} > 2m_\tau$  otherwise the decay of  $\phi_2$  will proceed via off-shell taus with a typical lifetime much bigger than the needed 30 ps. One consequence of such restricted kinematics is that the four  $\phi_2$  are non-relativistic in the rest frame of the parent  $\phi$ , with typical kinetic energy

$$E_{\text{kin}} = \frac{m_\phi}{4} - m_{\phi_2} \simeq (0.2 \div 0.7) \text{ GeV}.$$

As noticed in [7], this leads to  $\phi_2$  decay vertices collinearly aligned along the  $\phi$  momentum. Indeed, their typical separation  $\delta$  in the orthogonal direction is

$$\delta \sim \beta \cdot c\tau_0, \quad \beta \sim (2E_{\text{kin}}/m_{\phi_2})^{1/2} \simeq 0.3 \div 0.6. \quad (4.1)$$

Since we are here concerned only with muon tracks, the  $\phi_2$  decay vertices cannot be reconstructed in most cases. However, a nontrivial experimental measure of their collinear alignment can be defined purely in terms of muonic tracks, for events with at least 3 muons in a cone. We will use the following quantity:

$$A = \min_{\vec{p}} \left( \sum_i [d_i(\vec{p})]^2 \right)^{1/2}$$

where  $d_i$  is the distance between the track of the  $i$ -th muon and a straight line passing through the primary vertex in the direction  $\vec{p}$ . By tracks here we mean idealized reconstructed tracks, where the effects of bending in the magnetic field of the detector have been deconvoluted. Thus  $A = 0$  exactly when all tracks intersect a single line pointing to the primary vertex. Generically we expect  $A$  positive and of the order of Eq. (4.1), although this is likely to be an overestimate since the definition of  $A$  makes it automatically vanish for cones with only two muons.

In Fig. 8 we plot the simulated distribution of  $A$  of events with at least 3 muons in a cone. A less steep distribution, similar to the one of the impact parameter  $d$  in Fig. 6, would instead arise from non-aligned  $\tau$  decays. In Fig. 8 we assumed two values of the  $\phi$  mass: 15 and 17 GeV,  $m_{\phi_2} = 3.6$  GeV and  $m_{\phi_1} = 7.3$  GeV.

## 4.3 Deviation from back-to-backness

While the total muon momenta in each cone  $\vec{p}_{1,2}$  is only a fraction of their parent  $\phi$  momentum, so that the muon invariant mass gives a poor information on the  $\phi$  mass,  $\vec{p}_1$  is very strongly correlated to the direction of  $\phi$ , allowing to test details of the  $\phi$  production mechanism.

The distribution of  $\phi$ 's in rapidity does not contain much information, being mostly shaped by the experimental cuts and by the parton distributions. More interesting is the distribution of the relative azimuthal angle  $\Delta\varphi$  (i.e. the relative angle between  $\vec{p}_1$  and  $\vec{p}_2$  in the plane transverse to the beam), since the deviation from the back-to-back configuration ( $\Delta\varphi = \pi$ ) can be due only

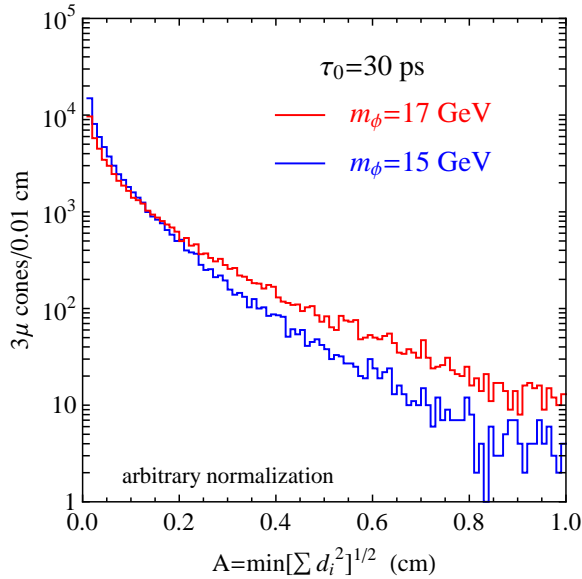


Figure 8: *Simulated distributions of the muon track alignment parameter  $A$ , for events with exactly 3 muons in a cone.*

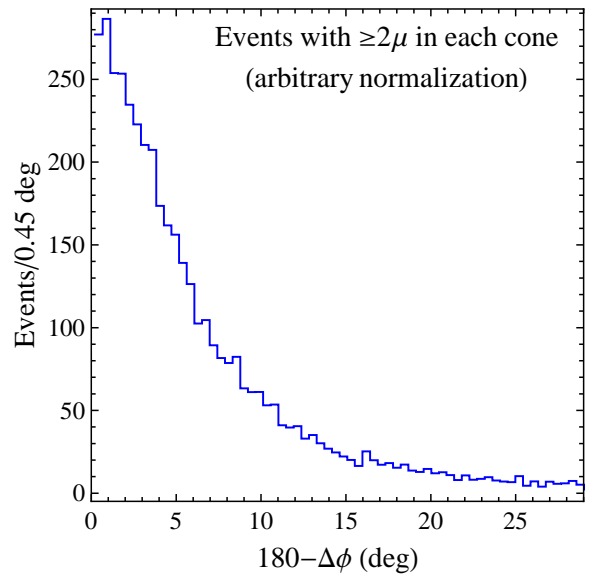


Figure 9: *The expected ‘deviation from back-to-backness’ angle  $\pi - \Delta\phi$  distribution for events with at least 2 muons in each cone.*

to QCD radiation in our model. In our model  $\phi$  is a color singlet, so that only Initial State Radiation is present, leading to small deviations from back-to-backness. Fig. 9 shows our result for the simulated distribution of  $\Delta\phi$  for signal events containing at least two muons in each cone: the average angle is

$$\langle 180^\circ - \Delta\phi \rangle \approx 7^\circ.$$

We relied on PYTHIA 8.108 with its standard settings of ISR parameters and no detector simulation, and we have not attempted to quantify QCD uncertainties on this result. Once these issues are settled, such distribution can discriminate from other production mechanisms or possible backgrounds. For instance,  $\phi$  production via the alternative gluon operator  $O_{6G}$  gives  $\sim 2$  times wider distribution since Initial State Radiation off gluons is stronger. A wider distribution would also be obtained in presence of *Final* State Radiation, which could be the case if the multi-muon events are background associated with dijet events. Indeed, analogous experimentally measured distributions for  $b\bar{b}$  production [10] are significantly wider.

## 5 Explicit realizations for $O_5$

We are not concerned here by the nature of the *hidden* world, and we do not pretend to *explain* the interaction that leads to the last step of the chain decay:  $\phi_2 \rightarrow \bar{\tau}\tau$ . Given its small width, we can attribute it to another effective operator

$$L_{\text{decay}} = \frac{1}{\Lambda'} \bar{l}_3 \tau H_s^c \phi_2 \quad (5.1)$$

where  $H_s$  is the standard Higgs field,  $l_3$  is the third-generation lepton doublet,  $\tau$  the singlet. The scale  $\Lambda'$  associated with it is much above the Fermi scale, unlike the  $\Lambda$  associated to  $\phi$ -production.

On the contrary, to be credible, the effective non-renormalizable operators in eq. (2.1) suppressed by a scale  $\Lambda$  as low as one hundred GeV must be “deconstructed” in terms of some explicit particle exchanges. What can mediate the pretty strong communication between the SM particles and the hidden world represented by  $\phi$  or the other light particles to which  $\phi$  decays, without running in conflict with known experimental constraints?

We concentrate our attention to  $O_5$ , leaving the two dimension-6 operators to Appendix A.

There are only two ways in which the operator  $O_5$  can be generated by the mediation of a single particle: 1) a scalar exchanged in the  $s$ -channel, with the quantum numbers of the standard Higgs doublet, but different from it and with a negligibly small vacuum expectation value; 2) a colored fermion exchanged in the  $t$ -channel. We analyze both cases in turn.

## 5.1 Scalar exchange

The renormalizable Lagrangian that gives rise to  $O_5$  after integrating out the heavy scalar doublet  $H$ , with hypercharge  $-1/2$ , is

$$L_H = \lambda_q \bar{q} u H + \lambda H^\dagger H_s |\phi|^2 - M_H^2 H^\dagger H, \quad (5.2)$$

where  $q$  is the first generation left-handed quark doublet and  $u$  is the right-handed up quark. (Similar considerations would hold for the down quark.) In this way, at energies below  $M_H$ , one generates an effective Lagrangian with  $O_5$  for the up quark and a scale

$$\Lambda = \frac{M_H^2}{\lambda_q \lambda v}, \quad (5.3)$$

which, to match with Fig. 1, should be about 100 GeV.

Requiring as the perturbativity limit that the partial width  $H \rightarrow \phi\phi^*$  be less than the  $H$  mass<sup>7</sup>, we get

$$\Gamma(H \rightarrow \phi\phi^*) \sim \frac{1}{16\pi} \frac{(\lambda v)^2}{M_H} < M_H \quad \implies \quad \lambda v < \sqrt{16\pi} M_H. \quad (5.4)$$

From the last two equations we conclude that

$$M_H/\lambda_q \lesssim 700 \text{ GeV}. \quad (5.5)$$

This bound applied to the Lagrangian (5.2) raises issues of potential conflicts with experiments, which we briefly address in Section 5.3. Here we focus on its possible effects at the Tevatron itself.

The first of these effects concerns the same  $p\bar{p} \rightarrow \phi\phi^*$  production, since the effective-operator approximation in describing the  $H$ -exchange may be invalid. This is illustrated in Fig. 10 where the effective-operator result of Fig. 1a is compared with the exchange of the  $H$ -scalar with a mass of 1 TeV and a width of 600 GeV. For these values of the parameters we see no conflict with the data, which may even be better described in the second case.

---

<sup>7</sup>For  $M_H < 3$  TeV this turns out to be stronger than the NDA bound  $\lambda < 16\pi^2$ .

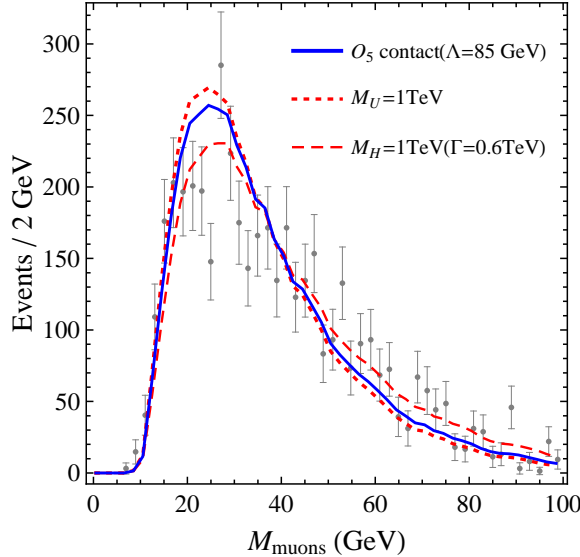


Figure 10: *The analogue of Fig. 1a where the contact term interaction generated by the local operator  $O_5$  is compared with a scalar  $s$ -channel effect and a fermion  $t$ -channel exchange generating the same operator at low energies. The couplings are slightly adjusted so that the total number of events is the same in all cases.*

Another effect of the  $H$ -exchange might have shown up in dijet properties. CDF has published studies both of the angular distribution of the dijets [8] and of a possible resonant structure in the dijet mass spectrum [9]. In both cases it is nontrivial for us to compare these results with the signal we might expect. For the case of the angular distribution, the  $H$ -exchange generates the operator

$$- \frac{\lambda_q^2}{2M_H^2} (\bar{u}u)^2, \quad (5.6)$$

whereas the analysis in [8] concerns the operator (including the sign)

$$- \frac{1}{2\Lambda^2} (\bar{q}_L \gamma^\mu q_L)^2, \quad q = (u, d)^T, \quad \Lambda > 700 \text{ GeV at 95\% C.L.} \quad (5.7)$$

The analysis leading to this bound is based on the fact that operator (5.7) interferes constructively with the QCD  $q\bar{q} \rightarrow q\bar{q}$  scattering amplitude, leading to an increase of events at large scattering angles. Our preliminary analysis shows that the interference term between the operator (5.6) and the QCD amplitude is smaller. Thus we expect that the bound in (5.5) should not pose a problem. All this is preliminary, however, also because the resonance may be within the accessible range. Indeed the same resonance search in [9] could be of importance to us. The problem in this case, however, is that the published limits concern only narrow resonances, when the width is within the resolution, while we are dealing with the opposite case. How to rescale from this, if possible at all, is to the least nontrivial. We believe however that the current results may only constrain  $M_H$  weakly enough to allow consistency with our effects in a significant range of the parameters.

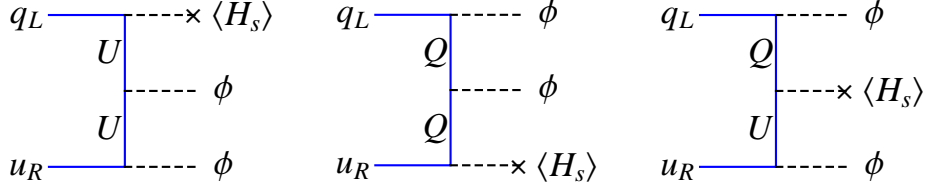


Figure 11: *Three ways to generate  $O_5$  via new heavy quark exchange in the  $t$ -channel. Only the last way, corresponding to the Lagrangian (5.9), is phenomenologically acceptable.*

## 5.2 Fermion exchange

The other way to generate the operator  $O_5$  is by a heavy quark exchange in the  $t$ -channel, see Fig. 11. In principle one can do it with one  $SU(2)_L$ -singlet  $U$  or with one doublet  $Q$ , but this requires large couplings of the form

$$\lambda_q \bar{q} U H_s, \quad \lambda_q \bar{Q} u H_s, \quad (5.8)$$

respectively for the  $U$  or the  $Q$  cases (here  $q$  is the standard SM left-handed doublet).

However, after diagonalization of the full mass matrix in the  $2/3$ -charge sector, this would lead to a large wrong component of the physical  $u_L^{\text{ph}}$  or  $u_R^{\text{ph}}$ , which is not acceptable. One needs therefore to introduce both a  $U$  and a  $Q$  and the Lagrangian

$$L_F = (\lambda_q \bar{q} Q \phi + \lambda_u \bar{U} u \phi^* + \lambda \bar{Q}_R U_L H_s + h.c.) + M_Q \bar{Q} Q + M_U \bar{U} U, \quad (5.9)$$

which, in the local limit and the approximations  $M_U \approx M_Q \gg \lambda v$ , gives rise to  $O_5$  with

$$\Lambda = \frac{M_U^2}{\lambda_q \lambda_u \lambda v}. \quad (5.10)$$

As in the case of a scalar exchange there are effects of non-locality, depending on the value of  $M_U \approx M_Q$ . The  $\hat{t}$  term in the  $t$ -channel fermion propagator,  $(\hat{t} - M_U^2)^{-1}$ , while negligible for small  $\hat{t}$ , suppresses the rate for events with the large invariant mass. The strength of this suppression can be estimated from  $\hat{t} \sim -\hat{s}/2$  (relevant for a  $\sim 90^\circ$  scattering angle). As discussed in Section 2,  $\hat{s} \sim 1$  TeV for events near the tail of the  $M_{\text{muons}}$  distribution in Fig. 1. Quantitatively, this effect is illustrated in Fig. 10 for  $M_U = 1$  TeV, showing that a much lower value of the heavy fermion mass would lead to a too strong depletion of the tail in the invariant mass distribution of the muons. To comply with  $\Lambda \approx 100$  GeV,  $M_U \gtrsim 1$  TeV requires therefore  $\lambda_q \lambda_u \lambda \gtrsim 60$ , i.e. a collection of pretty strong couplings.

The Lagrangian (5.9) generates also several 4-quark interactions at one loop, potentially relevant for the dijet physics. The typical scale of these operators will be  $\sim 4\pi\Lambda \approx 1.3$  TeV, which, as previously discussed, should be compatible with current limits.

### 5.3 Problems for a more complete theory

The formulation of a full proper extension of the SM that incorporates in a consistent way both the hidden and the mediation sectors, in one of the two versions above, would obviously be premature at this stage and, as such, is outside the scope of this work. Here we briefly mention some of the problem one would have to face. They are of at least three kinds:

1. Flavor problems;
2. Naturalness problems associated with the lightness of  $\phi$  (and the other hidden particles);
3. In the scalar-exchange case, a naturalness problem associated with the need of a vanishingly small vacuum expectation value of  $H$ .

The flavor problems are associated with the presence of the effective 4-quark interactions already discussed in connection with possible dijet signals. Even in the 2/3-charge sector the limits on the effective scale of these interactions, if not properly aligned in flavor space, are severe. One at least technically acceptable way out may consist in assuming that all the Yukawa interactions in  $L_H$ , Eq. (5.2), or  $L_F$ , Eq. (5.9), *and* in the SM be flavor diagonal *except* for the usual Yukawa coupling of the *down* quarks, which would therefore be the only source of flavor breaking.

The issue of the naturally small masses of the hidden sector scalars has a lot to do with their nature and their possible internal structure, about which little is known. Nevertheless it may be in any case nontrivial to accommodate in a natural picture their large Yukawa couplings as in (5.2) or in (5.9).

Finally, from (5.2) a non vanishing vacuum expectation value of  $H$  gives rise to contribution to the up quark mass,  $\delta m_u = \lambda_q \langle H \rangle$ , which needs to be kept under control. In turn, since  $\lambda_q$  cannot be too small, this is a severe limit on the mixing squared mass term  $m^2 H^\dagger H_s$  in the scalar potential. Seen another way, the operator  $O_5$  leads to a radiative contribution to the up quark mass from a  $\phi$  loop. This radiative correction could be removed, without affecting the multi muon signal, by replacing  $|\phi|^2 \rightarrow \phi^2$  in  $O_5$  and making proper adjustments in the deconstructed versions.

## 6 Dark matter connection?

Let us assume that the proposed interpretation of the CDF events is correct: a hidden sector with particles of mass of order 10 GeV, that decay into  $\tau$ 's and coupled to the Standard Model through new states  $Q, U$  or  $H$  with mass in the TeV region. Here we suppose that this TeV sector is augmented by a stable neutral state  $\chi$  that is the dark matter. To connect to the multi-muon data, we also assume that  $\chi$  is also strongly coupled to the hidden sector by the Yukawa interactions  $\chi\chi(\phi, \phi_1, \phi_2)$  for fermionic  $\chi$ , or the quartic couplings  $\chi^\dagger\chi(\phi^*\phi, \phi_1^*\phi_1, \phi_2^*\phi_2)$  for scalar  $\chi$ , so that the dominant dark matter annihilation channels are

$$\chi\chi \rightarrow \phi^*\phi, \phi_1^*\phi_1, \phi_2^*\phi_2 \rightarrow (\bar{\tau}\tau)^8, (\bar{\tau}\tau)^4, (\bar{\tau}\tau)^2. \quad (6.1)$$



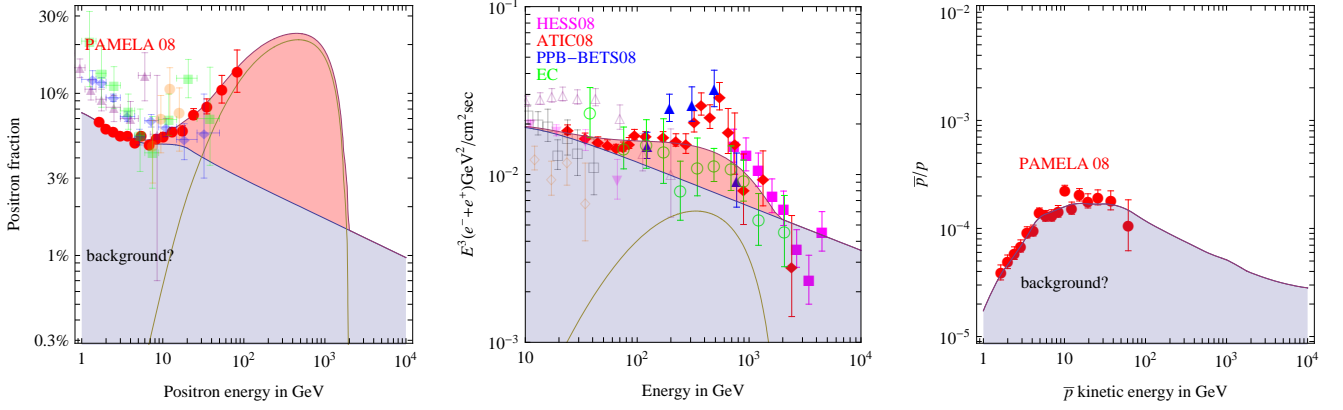


Figure 12: *The cosmic ray data about the positron fraction  $e^+/(e^+ + e^-)$  (left),  $e^+ + e^-$  (middle), anti-proton fraction  $\bar{p}/p$  (right) compared to the expected astrophysical backgrounds (lower shaded curve) plus the Dark Matter excess (upper red curve).*

If this annihilation cross section is large enough, the  $e^+$  from  $\tau$  decay are able to explain the excess positron cosmic ray signal reported by PAMELA [4], for  $m_\chi > (2, 1, 0.5)$  TeV, for dominant annihilations to  $\phi, \phi_1, \phi_2$  respectively. The predicted spectrum for the positron excess is shown in Fig. 12, that applies equally well to annihilation via  $\phi$  or  $\phi_1$  or  $\phi_2$  for  $m_\chi = (4, 2, 1)$  TeV, respectively. Since the kinematics is such that the  $\tau$  are produced non-relativistically in the rest frame of the decaying hidden sector scalar, the positron spectrum is similar in the three cases. A smoother spectrum arises if instead DM has more than one annihilation channel with comparable branching ratios. (See [11] and references therein for a discussion of the expected astrophysical backgrounds and uncertainties).

The connection with the CDF multi-muon data is that the signals involve  $\tau$  decays. As a consequence there is no associated  $\bar{p}$  excess, compatibly with PAMELA observations [4].

Future experiments measuring the positron excess at energies beyond 100 GeV should find that the excess persists smoothly to higher energies, with a turnover behavior, shown in Fig. 12, that is not as sharp as when annihilations occur directly to electrons or muons.

To obtain the PAMELA positron excess, the  $\chi\chi$  annihilation cross section must be larger than that required for a thermal freeze-out abundance of  $\chi$  by a boost factor

$$B \approx 10^3 \frac{m_\chi}{\text{TeV}}, \quad (6.2)$$

independent of whether the annihilation yields 2,4, or 8  $\bar{\tau}\tau$  pairs. A contribution to this boost factor arises from a Sommerfeld enhancement factor, from a ladder of  $\phi$  exchanges between the initial annihilating  $\chi$  states, and is significant since  $m_\phi \ll m_\chi$ . If  $\chi$  is a fermion the Yukawa coupling  $\chi\chi\phi$  leads to this ladder, while for  $\chi$  a scalar a new trilinear scalar coupling must be added,  $\chi\chi\phi$ . For the case of the Yukawa coupling,  $y\bar{\chi}(S + i\gamma_5 A)\chi$ , the desired thermal freeze-out abundance results if  $y^2 \approx m_\chi/1.5\text{TeV}$ . For  $m_\chi$  in the range of 1 to 10 TeV the Sommerfeld

enhancement factor is approximately given by

$$R \approx 200 \frac{m_\chi}{\text{TeV}}. \quad (6.3)$$

Comparing with (6.2), this is only a factor 5 below the required boost factor. Hence if local clumpiness of the halo provide the extra  $\approx 5$  enhancement, our theory is able to yield the PAMELA positron excess even with dark matter produced thermally. Such a local clumpiness is helpful in reducing tensions with limits on gamma [11] and neutrino fluxes.

In Fig. 12 we fixed the DM mass  $m_\chi$  trying to reproduce the peak suggested by the ATIC [5] observations of the  $e^+ + e^-$  spectrum below 1 TeV. However, the spectral feature produced via  $\tau$  decays (as suggested by the CDF anomaly) is less pronounced than that arising from DM annihilations to electrons or muons, so that higher statistics data will test the hypothesis of annihilations via  $\tau$  pairs.<sup>8</sup>

## 7 Conclusions

We explored the possibilities for a new-physics interpretation of the CDF multi-muon events, adopting the phenomenological conjecture of [3] which links the muons to the pair production of two hidden sector scalars, each decaying into 8  $\tau$  leptons. Within this conjecture we addressed the major puzzle left unexplained so far: a plausible production mechanism which could explain the total muon invariant mass spectrum. The hardness of this spectrum suggests to explore higher-dimension local operators connecting two quarks or gluons to a pair of  $\phi$ 's, and our systematic search revealed that one such operator, namely the dimension-5  $O_5 = \bar{q}q|\phi|^2/\Lambda$ , reproduces the measured distribution for  $\Lambda \simeq 100$  GeV.

Encouraged by this discovery, and by the ability to reproduce several other experimental distributions, we proceeded to discuss the next crucial question: is it at all conceivable that such a low scale can be generated in a more complete theory without producing any other unseen effect? We presented the two minimal ways of solving this problem, either by exchanging an  $s$ -channel new heavy scalar, or by exchanging a  $t$ -channel new heavy quark. In both cases 4-quark operators are unavoidably generated along with  $O_5$ , with a scale of the order a TeV. While the comparison with the existing Tevatron limits from dijet studies is nontrivial, our preliminary analysis shows that in both cases no obvious contradiction exists. Furthermore we found that the effects due to momentum dependence of the exchanged particle propagators may not disturb the agreement of the effective-operator limit with the total invariant mass distribution.

We think that all this offers a definite and consistent framework which can be subject to stringent tests by further comparison with the data. In fact, since the production mechanism is now largely fixed, it should be possible for the experimentalists to pronounce a final word on this model. We propose possible tests involving muons only; more tests involving hadronic tracks can be imagined.

---

<sup>8</sup>**Note Added.** The FERMI experiment [12] did not confirm the ATIC peak and observed an  $e^+ + e^-$  spectrum compatible with the model prediction in figure 12b.

If we assume that the proposed interpretation of the CDF events is correct, further work in many different directions can and must be done. Here we have not resisted from drawing a possible connection between the CDF data and the putative Dark Matter signals seen in PAMELA and/or ATIC. Assuming that Dark Matter is a hidden sector particle that annihilates into the  $\phi$ -scalars decaying into  $\tau$  leptons, we explored its indirect signals: one can reproduce the PAMELA  $e^+$  excess and, at higher energies, a feature in the  $e^+ + e^-$  spectrum milder than the one hinted at by the ATIC data.

## Acknowledgements

We are especially grateful to Paolo Giromini for many discussions and invaluable clarifications about the multi-muon CDF data. We thank Luciano Ristori and Michelangelo Mangano for discussions about the multi-muon events, and Gennaro Corcella for discussions about Monte-Carlo generators. R.B. and V.R. are partially supported by the EU under RTN contract MRTN-CT-2004-503369 and by MIUR under the contract PRIN-2006022501. The work of LH is supported by the U.S. Department of Energy under contract no. DE-AC02-05CH11231 and NSF grant PHY-04-57315.

## A Explicit realizations for $O_{6G}$ and $O_{6F}$

### A.1 Gluon operator

To *deconstruct*  $O_{6G}$  one needs at least one heavy quark singlet  $F$ , of mass  $M_F$  and unspecified charge, and the mediation coupling  $\lambda\phi\bar{F}F$ . Integrating it out at one loop gives rise to

$$L_{\text{eff}} \approx \frac{\lambda^2 g_s^2}{16\pi^2 M_F^2} O_{6G}, \quad (\text{A.1})$$

so that the threshold effect in Fig. 1b could be obtained with  $M_F \sim (\lambda/4\pi) \times 200$  GeV.

### A.2 Fermion operator

As in the case of  $O_5$ , there are two ways to generate  $O_{6F}$ , either by fermion or by heavy vector exchange. Concentrating on the vector-exchange case, the relevant gauge Lagrangian for a  $Z'$  of mass  $M$  could be

$$L = g_q Z'_\mu \sum_i \bar{q}_i \gamma_\mu q_i + g_\phi Z'_\mu (\phi^+ \overleftrightarrow{\partial}_\mu \phi) \quad (\text{A.2})$$

where  $i$  runs over all quarks. This can account for  $O_{6F}$ , with the needed effective scale to explain the tail of Fig. 1b, provided

$$M \approx (g_\phi/4\pi)^{1/2} \sqrt{g_q} 700 \text{ GeV}. \quad (\text{A.3})$$

At the same time, the  $Z'$ -width is dominated by decays into  $\phi\phi^*$  :

$$\Gamma \sim \frac{g_\phi^2}{48\pi} M. \quad (\text{A.4})$$

We believe that this leads to an acceptable situation, also in view of the dijet limits from CDF, provided  $g_\phi \rightarrow 4\pi$ . A model like this might be the easiest to incorporate in a complete extension of the SM.

## References

- [1] T. Aaltonen *et al.* [CDF Collaboration], “Study of multi-muon events produced in p-pbar collisions at  $\sqrt{s}=1.96$  TeV,” arXiv:0810.5357.
- [2] D0 Collaboration, arXiv:0906.2969. See also F. Happacher, talk at DIS 2009 (Madrid), [http://www-cdf.fnal.gov/physics/talks\\_transp/2009/happacher\\_dis2009.pdf](http://www-cdf.fnal.gov/physics/talks_transp/2009/happacher_dis2009.pdf), for a discussion of possible caveats in the D0 result.
- [3] P. Giromini *et al.*, “Phenomenological interpretation of the multi-muon events reported by the CDF collaboration,” arXiv:0810.5730.
- [4] PAMELA collaboration arXiv:0810.4995, arXiv:0810.4994.
- [5] ATIC collaboration, Nature 456 (2008) 362.
- [6] T. Sjöstrand, S. Mrenna and P. Skands, JHEP05 (2006) 026, arXiv:0710.3820
- [7] M. J. Strassler, “Flesh and Blood, or Merely Ghosts? Some Comments on the Multi-Muon Study at CDF,” arXiv:0811.1560.
- [8] The CDF Collaboration, “Search for Quark Substructure in the angular distribution of dijets produced in ppbar collisions at  $\sqrt{s}=1.96$  TeV,” (CDF/ANAL/JET/PUB/9609), [http://www-cdf.fnal.gov/physics/new/qcd/dijetchi\\_08/](http://www-cdf.fnal.gov/physics/new/qcd/dijetchi_08/)
- [9] T. Aaltonen *et al.* [CDF Collaboration], “Search for new particles decaying into dijets in proton-antiproton collisions at  $\sqrt{s} = 1.96$  TeV,” arXiv:0812.4036. See also CDF note 9246 with the same title.
- [10] T. Aaltonen *et al.* [CDF Collaboration], “Measurement of correlated b-bbar production in  $p\bar{p}$  collisions at  $\sqrt{s} = 1960$  GeV,” Phys. Rev. D **77**, 072004 (2008), arXiv:0710.1895.
- [11] G. Bertone, M. Cirelli, A. Strumia, M. Taoso, arXiv:0811.3744.
- [12] FERMI/LAT collaboration, arXiv:0905.0025.